

# Stepwise Iodide-Free Methanol Carbonylation via Methyl Acetate Activation by Pincer Iridium Complexes

Changho Yoo and Alexander J. M. Miller\*



Cite This: <https://doi.org/10.1021/jacs.1c05185>



Read Online

ACCESS |



Metrics & More

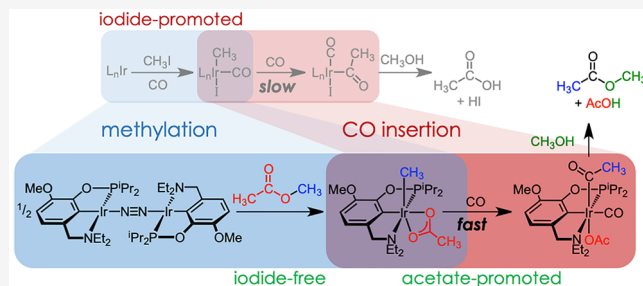


Article Recommendations



Supporting Information

**ABSTRACT:** Iodide is an essential promoter in the industrial production of acetic acid via methanol carbonylation, but it also contributes to reactor corrosion and catalyst deactivation. Here we report that iridium pincer complexes mediate the individual steps of methanol carbonylation to methyl acetate in the absence of methyl iodide or iodide salts. Iodide-free methylation is achieved under mild conditions by an aminophenylphosphinite pincer iridium(I) dinitrogen complex through net C–O oxidative addition of methyl acetate to produce an isolable methyliridium(III) acetate complex. Experimental and computational studies provide evidence for methylation via initial C–H bond activation followed by acetate migration, facilitated by amine hemilability. Subsequent CO insertion and reductive elimination in methanol solution produced methyl acetate and acetic acid. The net reaction is methanol carbonylation to acetic acid using methyl acetate as a promoter alongside conversion of an iridium dinitrogen complex to an iridium carbonyl complex. Kinetic studies of migratory insertion and reductive elimination reveal essential roles of the solvent methanol and distinct features of acetate and iodide anions that are relevant to the design of future catalysts for iodide-free carbonylation.



## INTRODUCTION

The production of acetic acid by methanol carbonylation is currently one of the largest scale industrial processes based on homogeneous catalysis, with annual capacity exceeding 13 million tons.<sup>1,2</sup> Iodide salts or methyl iodide are essential promoters in the catalytic reaction. Hydroiodic acid and methyl iodide are continually generated *in situ* during the process, with the latter initiating the organometallic catalytic cycle by forming a metal–methyl species (Scheme 1).<sup>3–5</sup> However, the need for iodide leads to serious disadvantages. Methyl iodide and hydroiodic acid are toxic and corrosive, necessitating expensive safety and engineering controls.<sup>4,6</sup> Iodide also complicates the chemical pathways. In the rhodium-catalyzed (“Monsanto”) process, the precipitation of RhI<sub>3</sub> is a significant catalyst deactivation pathway.<sup>4–6</sup> In the iridium-catalyzed (“Cativa”) process, iodide inhibits CO migratory insertion by generating inactive iodide-bound species, necessitating the use of halide abstractors such as ruthenium(II) salts to achieve high activity.<sup>4–7</sup> Therefore, development of low-iodide or iodide-free processes has attracted the attention of both academic and industrial scientists. Advances in iodide-free carbonylation have been driven by heterogeneous Lewis acid catalysts.<sup>8–16</sup> While promising, these systems typically require temperatures of ca. 200 °C and produce dimethyl ether as an undesired byproduct. Homogeneous molecular catalysts for methanol carbonylation without iodide promoters remain elusive.

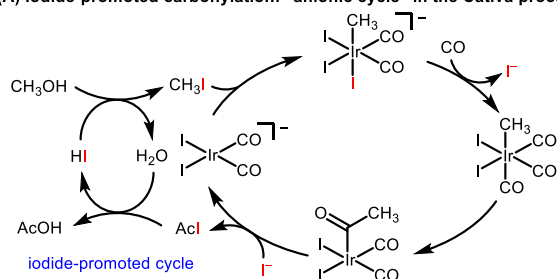
The primary challenge in halide-free carbonylation with molecular catalysts is accessing the organometallic methyl complexes that mediate C–C bond formation. Most catalysts must rely on potent alkylating agents such as methyl iodide to form the M–CH<sub>3</sub> unit (Scheme 1A). One strategy to minimize methyl iodide concentrations utilizes quaternary ammonium iodide or phosphonium iodide salts that produce only equilibrium amounts of methyl iodide under the reaction conditions of carbonylation.<sup>17</sup> Iodide is still required, however, and many of the concerns noted above remain in these systems.

An alternative approach involves designing organometallic catalysts capable of C–O oxidative addition (Scheme 1B), avoiding the need for H<sub>3</sub>C–I oxidative addition altogether. The most obvious and ideal reactant would be CH<sub>3</sub>OH, but we are not aware of any well-defined C–O oxidative addition reactions of methanol. We hypothesized that methyl acetate (MeOAc) could be a more promising candidate than methanol for halide-free alkylation because acetate is a better leaving group than hydroxide. Methyl acetate is also a coproduct and

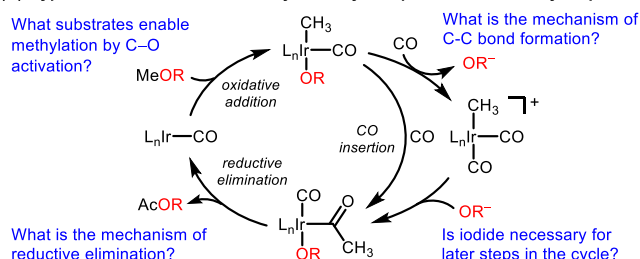
Received: May 19, 2021

### Scheme 1. Comparison of a Carbonylation Process Using Iodide and a Possible Iodide-Free Process via C–O Activation

(A) Iodide-promoted carbonylation: "anionic cycle" in the Cativa process



(B) Hypothetical iodide-free carbonylation cycle: questions about key steps



common solvent for methanol carbonylation.<sup>1–4</sup> However, examples of methyl acetate C<sub>sp</sub><sup>3</sup>–O bond cleavage are extremely limited and generally produce product mixtures.<sup>18–21</sup> In an encouraging example, the Goldman group showed that initial C–H bond activation at an iridium center initiates net C<sub>sp</sub><sup>3</sup>–O oxidative addition of methyl acetate.<sup>21</sup> However, the reaction required prolonged heating at 125 °C and suffered from unwanted C–H activation of *tert*-butyl substituents of the tertiary phosphine donor, precluding isolation of the methyliridium acetate product.

Our group previously reported catalytic methanol carbonylation using aminophenylphosphinite (NCOP) pincer iridium

complexes in the presence of methyl iodide and metal salt promoters.<sup>22</sup> Although partial dissociation of the ligand was observed under catalytic conditions, stoichiometric studies established the viability of each reaction step, including Lewis acid promotion of the C–C bond-forming migratory insertion step.<sup>23</sup> We recently isolated a NCOP iridium(I)–dinitrogen compound and found that it facilitates decarbonylative C–O bond cleavage of ethers, initiated by C–H bond activation.<sup>24</sup> These results led us to a stepwise study of iodide-free methanol carbonylation using methyl acetate as the methylating reagent. Here, the aminophenylphosphinite ligand supports clean formal oxidative addition of methyl acetate to generate an isolable methyliridium acetate complex. The subsequent migratory insertion and reductive elimination steps could then be studied individually, enabling a detailed understanding of how iodide-free conditions with acetate ions compared to conditions with iodide ions (helping to address the questions in Scheme 1B). The elimination process, in particular, has previously eluded careful interrogation in iridium-catalyzed carbonylation, leading to conflicting views on whether C–O or C–I bond formation occurs from the acetyl intermediate in the Cativa process.<sup>3,25–27</sup> The present study provides a rare opportunity to directly compare acetyl complex reactivity by either methanolysis to generate methyl acetate directly or reductive elimination with iodide to generate acetyl iodide as an intermediate.

## RESULTS AND DISCUSSION

**MeOAc Activation.** Initial studies investigating the activation of MeOAc by previously reported (NCOP)Ir(CO) complexes did not show promising reactivity, despite the ability of these carbonyl complexes to carry out the individual steps and overall catalytic reaction of methanol carbonylation in the presence of methyl iodide.<sup>22,23</sup> Inspired by reports from the Goldman group demonstrating net C–O bond activation via initial C–H bond activation,<sup>21,28–30</sup> and our own recent observation of ether decarbonylation via C–H bond

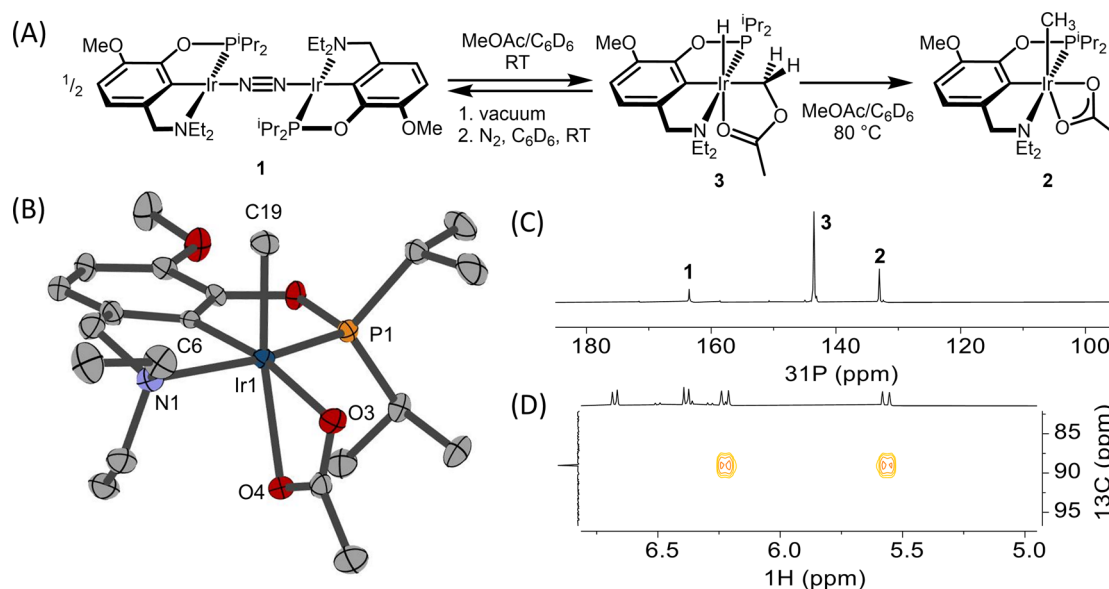


**Figure 1.** (A) MeOAc activation by **1** via C–H activation. (B) Structural representation of **2**. (C) <sup>31</sup>P{<sup>1</sup>H} NMR spectrum after reaction of **1** and MeOAc at room temperature for 24 h. (D) Partial <sup>1</sup>H–<sup>13</sup>C HSQC spectrum of **3** showing correlation of geminal protons with the carbon in an acetoxy methyl (–CH<sub>2</sub>OAc) group.

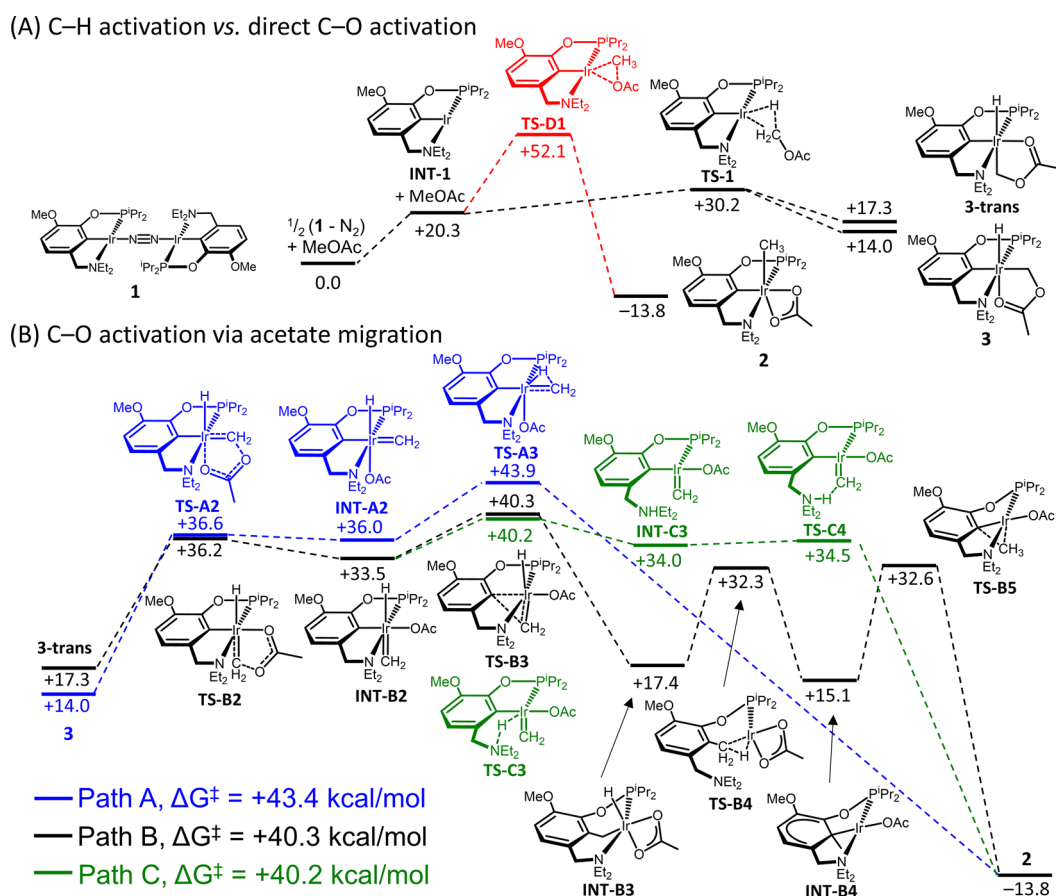


**Figure 2.** Calculated Gibbs free energies (kcal/mol) for reaction of **1** with MeOAc via C–H activation (blue, black, and green) and direct C–O activation (red). Values of  $G$  are given relative to  $\frac{1}{2}(\mathbf{1} - \mathbf{N}_2) + \text{MeOAc}$ . The free energies correspond to a reference state of 1 M concentration for each species participating in the reaction and  $T = 298.15$  K.

activation,<sup>24</sup> we turned to the dinitrogen complex  $[(^{\text{MeO-Et}}\text{NCOP})\text{Ir}]_2(\mu\text{-N}_2)$  (**1**).

A red solution of **1** and 1 equiv of MeOAc in benzene became colorless after heating at 80 °C for 1 h. NMR spectroscopy revealed 75% yield of a new species with a  $^{31}\text{P}\{^1\text{H}\}$  NMR signal ( $\delta$  133.36) upfield shifted from that of **1** ( $\delta$  163.68). A diagnostic upfield methyl resonance in the  $^{13}\text{C}\{^1\text{H}\}$  NMR spectrum ( $\delta$  –29.47, d,  $J_{\text{PC}} = 6.7$  Hz) supports the formation of the iridium methyl acetate complex  $(^{\text{MeO-Et}}\text{NCOP})\text{Ir}(\text{CH}_3)(\text{OAc})$  (**2**) (Figure 1A). Compound **2** was isolated in 42% yield after crystallization from diethyl ether at –35 °C. An X-ray diffraction (XRD) study revealed pseudo-octahedral Ir coordination with the methyl group *cis* to the pincer phenyl ligand and the acetate ligand in a bidentate ( $\kappa^2$ ) binding mode (Figure 1B).

Monitoring the conversion of **1** to **2** by NMR spectroscopy at room temperature revealed an intermediate. In  $\text{C}_6\text{D}_6$ , the reaction of **1** with 1 equiv of MeOAc was slow ( $\sim 60\%$  conversion of **1** in 10 h at room temperature) and resulted in multiple species along with trace amounts of **2**. When the reaction was instead conducted in a 1:1 mixture of MeOAc: $\text{C}_6\text{D}_6$  ( $\sim 110$  equiv of MeOAc relative to **1**) at room temperature, however, a prominent new  $^{31}\text{P}$  resonance grew in at  $\delta$  143.52 (Figure 1C). The intermediate **3** features a hydride resonance at  $\delta$  –26.11 (d,  $J_{\text{PH}} = 28.6$  Hz) in the  $^1\text{H}$  NMR spectrum, indicating a weak donor *trans* to the hydride.  $^1\text{H}$ – $^{13}\text{C}$  HSQC and HMBC NMR experiments enabled assignment as  $(^{\text{MeO-Et}}\text{NCOP})\text{Ir}(\text{H})(\kappa^2\text{C}, \text{O-CH}_2\text{OAc})$  (**3**, Fig-

ure 1A and Figures S4–S8). The  $\text{CH}_2\text{OAc}$  group was identified by the two diastereotopic geminal protons at  $\delta$  6.23 and  $\delta$  5.57 (d,  $^1J_{\text{HH}} = 11.3$  Hz) and  $^{13}\text{C}$  resonance at  $\delta$  89.49 (Figure 1D). After 24 h at room temperature, a mixture of **1** (10%), **3** (70%), and **2** (20%) was obtained (Figure 1C). Heating this reaction mixture at 80 °C for 1 h resulted in complete consumption of **1** and **3** to produce **2** in 75% yield. If, instead of heating, a similarly obtained mixture containing **1**, **2**, and **3** was exposed to vacuum to remove the MeOAc, only **1** and **2** remained after the solids were redissolved in  $\text{C}_6\text{D}_6$  under  $\text{N}_2$ . The formation of **3** from **1** is therefore a reversible process, while the formation of **2** is not.

The net C–O oxidative addition of methyl acetate mediated by the  $(^{\text{MeO-Et}}\text{NCOP})\text{Ir}$  center is noteworthy for proceeding in high yield under relatively mild conditions. For comparison, MeOAc activation by a diphosphine-based iridium pincer complex utilized by Goldman et al. required heating at 125 °C due to formation of a stable intermediate in which methylene inserts into the iridium–aryl bond of the pincer backbone.<sup>21</sup> Under the reaction conditions required to finally reach the methyliridium acetate complex, there is a competing side reaction involving C–H bond activation of a *tert*-butylphosphine substituent, preventing isolation of  $(^{\text{tBu}^4}\text{PCP})\text{Ir}(\text{Me})(\text{OAc})$  ( $^{\text{tBu}^4}\text{PCP}$  is 2,6- $(^{\text{tBu}}\text{PCH}_2)_2\text{-C}_6\text{H}_3$ ). In contrast, the present complex **2** is generated even at room temperature, is produced in high yield at 80 °C according to NMR spectroscopy, and can be isolated in a thermally stable crystalline form.

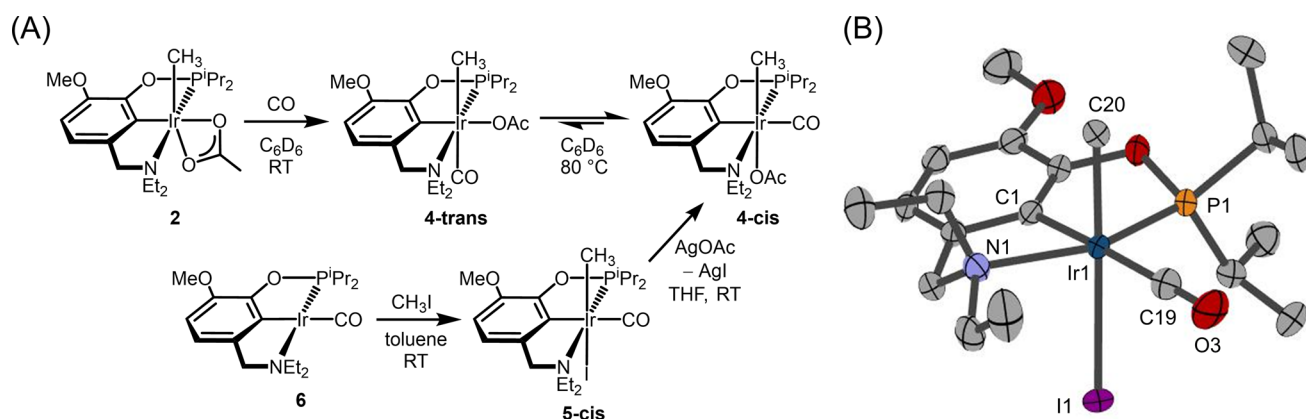


**Figure 3.** (A) Synthesis of carbonyl species. (B) Structural representation of **5-cis** from X-ray diffraction analysis, with ellipsoids drawn at 50% probability level. Hydrogen atoms are omitted for clarity.

To understand why the aminophenylphosphinite pincer ligand supports cleaner reactivity under milder conditions, the detailed mechanism of net C–O oxidative addition was examined by using density functional theory (DFT). Four pathways were considered: direct C–O oxidative addition and three pathways that start with C–H bond activation (Figure 2). The experimental observation of alkyl hydride intermediate **3** provides strong evidence against a direct C–O oxidative addition pathway, instead supporting initial oxidative addition of a C–H bond of MeOAc (Figure 1A). Accordingly, the barrier to C–H activation was computed to be ca. 30 kcal/mol while the barrier to direct C–O oxidative addition was computed to be 52.1 kcal/mol.

Possible C–H activation routes were evaluated in detail through DFT calculations (Figure 2). Paths A, B, and C all start with N<sub>2</sub> dissociation and C–H activation by the coordinatively unsaturated intermediate INT-1. The resulting hydride species **3** is higher in energy than **1** ( $\Delta G = +14.0$  kcal/mol) due to unfavorable N<sub>2</sub> dissociation ( $\Delta G = +20.3$  kcal/mol). However, in experimental practice the reaction may be driven by low N<sub>2</sub> solubility at the elevated temperature and/or the excess amount of MeOAc, consistent with our experimental observation of equilibrium formation of **3** with ~110 equiv of MeOAc at room temperature.

In path A, alkyl hydride **3** undergoes acetate migration to produce an intermediate with a methylidene ligand *cis* to the hydride (INT-A2), likely by retro-electrocyclization (TS-A2,  $\Delta G^\ddagger = +36.6$  kcal/mol). The methyl species **2** can be generated by 1,1-hydride migration (TS-A3,  $\Delta G^\ddagger = +43.9$  kcal/mol), which has the highest activation barrier in the overall reaction.

In Path B, C–H bond activation produces **3-trans**, in which the acetoxymethyl carbon (–CH<sub>2</sub>OAc) is *trans* to hydride ( $\Delta G = +3.3$  kcal/mol relative to **3**). Both **3-trans** and **3** are accessed by the same early C–H activation transition state TS-1, with barrierless coordination of oxygen either *cis* or *trans* to the hydride producing the respective isomers of **3** (Figures S46 and S47). Complex **3-trans** could also form by isomerization of **3**, either via TS-1 ( $\Delta G = +16.2$  kcal/mol relative to **3**) or via oxygen dissociation, bending of the Ir–CH<sub>2</sub>OAc bond, and recoordination of oxygen ( $\Delta G < 14$  kcal/mol based on the potential energy surface scan, Figure S48). The subsequently formed *trans*-methylidene (INT-B2) cannot undergo direct C–H reductive elimination with hydride, so it is first inserted into the Ir–C<sub>aryl</sub> bond to give INT-B3. This process has the

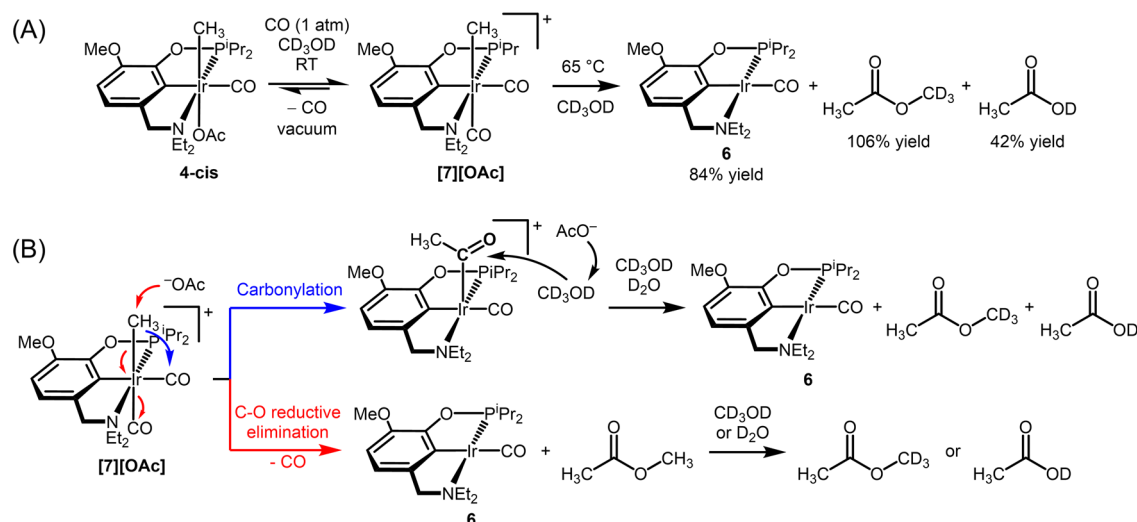
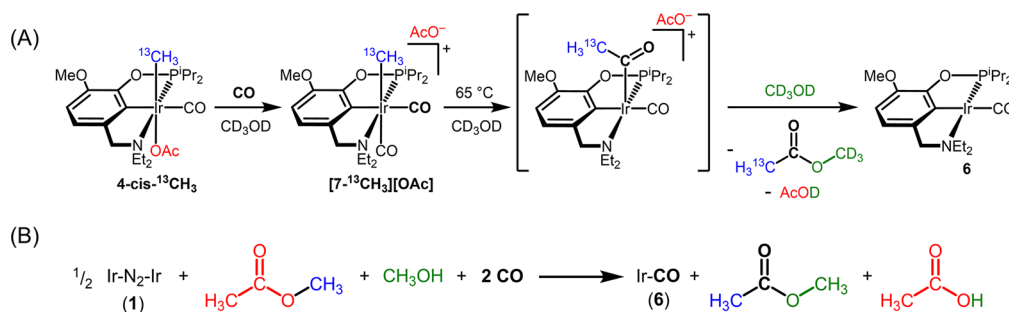
highest energy TS in path B (TS-B3,  $\Delta G^\ddagger = +40.3$  kcal/mol). The subsequent C–H reductive elimination yields INT-B4, in which the methyl from methyl acetate is added on the aromatic backbone of the NCOP ligand. In the transition state (TS-B4), the amine donor is dissociated, enabling a geometric distortion that facilitates concerted reductive elimination between adjacent hydride and ArCH<sub>2</sub> ligands. Finally, the C–C oxidative addition of the Ar–CH<sub>3</sub> bond in INT-B4 produces the methyl species **2**.

In path C, the amine arm acts as a proton relay. From *trans*-methylidene intermediate INT-B2, Ir–N bond cleavage and N–H bond formation occur (i.e., amine deprotonation of the hydride ligand) to give INT-C3. The ammonium group then transfers the proton to the methylidene ligand to form the methyl species **2**. The highest activation barrier is deprotonation of hydride by the amine (TS-C3,  $\Delta G^\ddagger = +40.2$  kcal/mol).

All pathways involving initial C–H activation (paths A, B, and C, Figure 2) are plausible based on the computational data and have significantly lower computed activation barriers than the direct C–O bond activation (path D). The slightly lower overall free energy spans for paths B and C relative to path A are attributed to hemilability of the amine donor of the pincer ligand. A mechanism akin to path B was proposed in C–O and C–C bond activation by diphosphine-based pincer rhodium and iridium complexes;<sup>21,31–33</sup> however, a higher barrier is encountered in the (<sup>t</sup>Bu<sup>4</sup>PCP)Ir analogue to TS-B4.<sup>21</sup> The lower barrier of TS-B4 for the (NCOP)Ir system is ascribed to amine hemilability. Whereas no phosphine dissociation was apparent in calculations of the (<sup>t</sup>Bu<sup>4</sup>PCP)Ir system, thus requiring an isomerization sequence before reductive elimination, the (NCOP)Ir system does not require any geometric isomerization, and instead amine dissociation is apparent in TS-B4 (Figure 2), which would provide increased flexibility for low-barrier C–H reductive elimination. Path C also features a relatively low-barrier pathway enabled by a labile amine donor acting as a hydride-to-methylidene proton shuttle. Hemilability of the amine donor may therefore be responsible for the relatively low barriers and thus the clean reactivity of the (NCOP)Ir complex under mild conditions compared to the (<sup>t</sup>Bu<sup>4</sup>PCP)Ir system.

Having identified a clean methylation reaction involving methyl acetate, we individually examined CO migratory insertion and acetyl reductive elimination steps.

**CO Migratory Insertion.** Addition of 1 atm of CO to a solution of methyliridium acetate complex **2** at room

Scheme 2. (A) Carbonylation of 4-cis in CD<sub>3</sub>OD; (B) Possible Routes for Formation of 6 and Acetyl ProductsScheme 3. (A) Isotopic Labeling Experiment of 4-cis-<sup>13</sup>CH<sub>3</sub> Carbonylation; (B) The Overall Net Reaction of Methanol Carbonylation by Pincer Complexes

temperature in C<sub>6</sub>D<sub>6</sub> immediately produced the carbonyl complex (<sup>MeO-Et</sup>NCOP)Ir(CH<sub>3</sub>)(OAc)(CO) (**4-trans**, where **trans** indicates the relative orientation of the carbonyl and methyl ligands). The methyl resonance was found at  $\delta$  0.71 in the <sup>1</sup>H NMR spectrum. Heating a solution of **4-trans** at 80 °C in C<sub>6</sub>D<sub>6</sub> under CO produced a new species with a methyl resonance shifted to  $\delta$  0.47. The new species was assigned as the isomer (<sup>MeO-Et</sup>NCOP)Ir(CH<sub>3</sub>)(CO)(OAc) (**4-cis**, Figure 3A). The <sup>13</sup>C{<sup>1</sup>H} NMR spectrum of **4-cis** confirms the presence of a CO ligand ( $\delta$  185.36) and a methyl ligand ( $\delta$  -30.92, d,  $J_{PC}$  = 7.2 Hz). The infrared (IR) spectrum of **4-cis** is consistent with a single carbonyl ligand ( $\nu_{CO}$  = 2023 cm<sup>-1</sup>) and a monodentate acetate ligand ( $\nu_{C=O}$  = 1622 cm<sup>-1</sup>,  $\nu_{C-O}$  = 1316 cm<sup>-1</sup>). After 36 h heating at 80 °C, the ratio of **4-trans**:**4-cis** was 1:10. Higher purity samples of **4-cis** could be obtained from the reaction of (<sup>MeO-Et</sup>NCOP)Ir(CO) (**6**) with CH<sub>3</sub>I to produce (<sup>MeO-Et</sup>NCOP)Ir(CH<sub>3</sub>)(CO)(I) (**5-cis**), followed by iodide abstraction with AgOAc (Figure 3). Heating a solution of pure **4-cis** under N<sub>2</sub> in C<sub>6</sub>D<sub>6</sub> at 80 °C produced a mixture of **4-trans** and **4-cis**, with a similar ratio as observed when after heating **4-trans**, confirming that the two isomers are in equilibrium ( $\Delta G$  = -1.6(1) kcal/mol favoring formation of **4-cis**). DFT calculations also predict that **4-cis** is thermodynamically favored over **4-trans** ( $\Delta G$  = -2.9 kcal/mol in the gas phase).

No CO migratory insertion to form an acetyl product was observed during thermolysis of **4-cis** under CO in C<sub>6</sub>D<sub>6</sub>. Similarly, refluxing solutions of **4-cis** in CD<sub>2</sub>Cl<sub>2</sub> or CD<sub>3</sub>CN

under 1 atm of CO overnight resulted in no C-C bond formation. Trace amounts of (<sup>MeO-Et</sup>NCOP)Ir(CO) (**6**) were the only new product observed.

Reactions in methanol, however, tell a different story (Scheme 2). Addition of 1 atm of CO to a solution of **4-cis** in CD<sub>3</sub>OD at ambient temperature resulted in formation of a new methyl species (<sup>31</sup>P{<sup>1</sup>H} NMR  $\delta$  141.93) in ~70% yield within 5 h. New methyl resonances (<sup>1</sup>H NMR  $\delta$  0.60, d,  $J_{PH}$  = 2.0 Hz and <sup>13</sup>C{<sup>1</sup>H} NMR  $\delta$  -9.21, d,  $J_{PC}$  = 6.2 Hz) were found slightly downfield of those in **4-cis**. Two carbonyl carbon resonances were found at  $\delta$  173.17 and 168.75 in the <sup>13</sup>C NMR spectrum, indicating that the new product is a methyl dicarbonyl complex with an outer-sphere acetate counteranion, [(<sup>MeO-Et</sup>NCOP)Ir(CH<sub>3</sub>)(CO)<sub>2</sub>][OAc] ([7]-[OAc], Scheme 2). Monitoring the reaction over 18–22 h did not lead significant changes in the ratio of products, suggesting that the reaction achieved equilibrium ( $K_{eq}$  = 24.0(3),  $\Delta G$  = -1.88(1) kcal/mol).

Heating a solution of [7][OAc] in CD<sub>3</sub>OD under 1 atm of CO at 65 °C led to complete conversion to the carbonyl complex **6** (84% yield) after 2 days, with concomitant production of partially deuterated methyl acetate CH<sub>3</sub>COOCD<sub>3</sub> (<sup>1</sup>H NMR  $\delta$  2.02, 106% yield) and acetic acid CH<sub>3</sub>COOD (<sup>1</sup>H NMR  $\delta$  1.92, 42% yield) (Scheme 2A). The partially deuterated methyl acetate could form upon reductive elimination of acetyl with CD<sub>3</sub>OD solvent or upon reductive elimination of methyl and acetate groups from [7][OAc] (without formation of the acetyl intermediate)

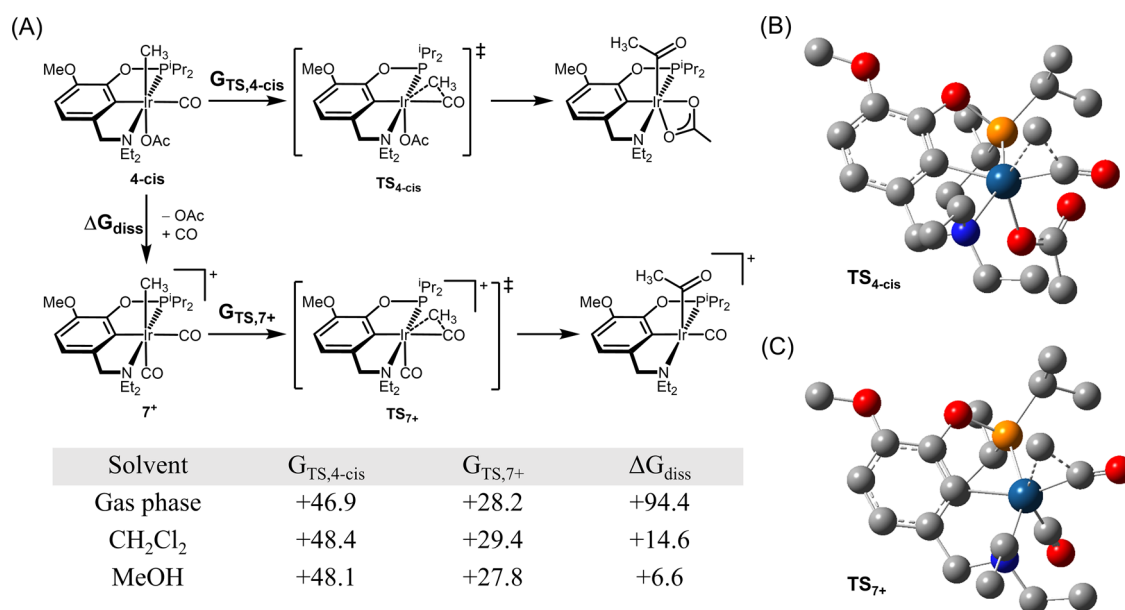


**Figure 4.** Calculated transition state energy (free energies in kcal/mol) for CO insertion in 4-cis and  $[7]^+$  and acetate dissociation energy (A). Calculated transition state structures for migratory insertion in 4-cis (B) and  $[7]^+$  (C).

followed by transesterification of methyl acetate with  $CD_3OD$  solvent (Scheme 2B). In the former case, a total of 2 equiv of acetyl products ( $CH_3COOCD_3 + CH_3COOD$ ) would be formed, whereas only 1 equiv is expected in the latter case (Scheme 2B). The formation of  $\sim 1.5$  equiv of acetyl products indicates acetyl formation via carbonylation. To confirm the origin of the acetic acid and methyl acetate products, an isotopic labeling experiment was performed.

Reaction of **6** with  $^{13}CH_3I$ , followed by iodide abstraction with  $AgOAc$ , afforded the  $^{13}C$ -labeled methyl complex ( $^{MeO-Et}NCOP$ )Ir( $^{13}CH_3$ )(CO)(OAc) (**4-cis- $^{13}C$** ). After heating a  $CD_3OD$  solution of **4-cis- $^{13}C$**  at 65 °C under 1 atm of CO for 18 h, a  $^{13}C$ -enriched signal was detected at  $\delta$  20.48 in the  $^{13}C$  NMR spectrum, with a corresponding doublet ( $\delta$  2.02,  $^1J_{CH} = 129.4$  Hz) in the  $^1H$  NMR spectrum indicating the formation of labeled methyl acetate  $^{13}CH_3COOCD_3$  by carbonylation and elimination of acetyl with  $CD_3OD$  (Scheme 3A). The reaction is balanced by proton transfer from methanol to acetate, forming acetic acid without  $^{13}C$  enrichment,  $CH_3COOD$  ( $^1H$  NMR  $\delta$  1.95, s), as a coproduct. Because **4-cis** can be produced from the activation of methyl acetate followed by CO addition, the overall reaction is methanol carbonylation to acetic acid using methyl acetate as a methylating promoter (Scheme 3B).

**Solvent Effects on CO Insertion: Facilitating Acetate Dissociation.** The acceleration of migratory insertion by methanol solvent has been observed with the Cativa catalyst.<sup>34</sup> Similarly, the carbonylation of methyl complex **4-cis** was only observed in methanol solution. Given that methanol was the only solvent in which CO substituted the acetate ligand in **4-cis**, we hypothesized that formation of cationic dicarbonyl species  $[7]^+$  was key for CO migratory insertion. The DFT-calculated transition state energies for CO migratory insertion in **4-cis** and  $[7]^+$  are compared in Figure 4A. Both transition state structures are consistent with the usual mechanism of methyl migration to the CO ligand (Figure 4B,C). The barrier for neutral acetate species **4-cis** is high ( $G_{TS,4-cis} = +48.1$  kcal/mol); the migratory insertion barrier for cationic dicarbonyl  $[7]^+$  is ca. 20 kcal/mol lower ( $G_{TS,7^+} = +27.8$  kcal/mol). The

cationic species is expected to possess a more electrophilic CO ligand, facilitating nucleophilic attack by the methyl ligand.<sup>7,35</sup> In addition, the methyl group in  $[7]^+$  may be more nucleophilic due to the strong *trans* influence of the carbonyl ligand relative to acetate. Support for this notion comes from comparisons (Table S13) of calculated Ir–CH<sub>3</sub> bond distances in  $[7]^+$  (2.14 Å) vs **4-cis** (2.11 Å) and comparisons of NBO charges on the methyl carbon in  $[7]^+$  (−0.80) vs **4-cis** (−0.77). The NBO charge on the carbonyl carbon is similar in magnitude but opposite in sign, consistent with a more electrophilic CO ligand in  $[7]^+$  compared to **4-cis**.

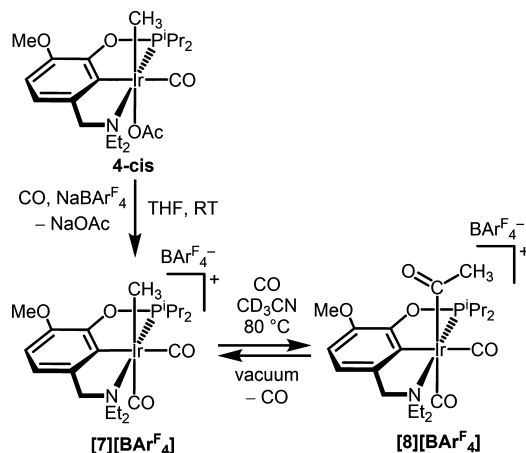
The calculations suggest methanol solvation does not significantly impact the CO insertion barrier for either **4-cis** or  $[7]^+$  (Figure 4A). Instead, we propose that the primary role of the methanol solvent is to promote pre-equilibrium acetate dissociation through dipole and hydrogen-bonding interactions. The calculations agree that substitution of acetate by CO is more accessible in methanol ( $\Delta G_{diss} = +6.6$  kcal/mol) than in  $CH_2Cl_2$  (+14.6 kcal/mol) (Figure 4A). The experimental data show that the acetate dissociation and CO binding is slightly exergonic ( $\Delta G_{diss} = -1.88(1)$  kcal/mol), which is in reasonable agreement with DFT when considering that the calculations do not account for explicit solvent interactions such as hydrogen-bonding interactions between the methanol solvent and acetate anion.

The DFT calculations suggests that generation of a cationic species is important for CO migratory insertion. This is consistent with a body of experimental evidence that relatively electron-deficient cationic alkyl carbonyl complexes undergo fast migratory insertion.<sup>7,35</sup> For example, iodide inhibits CO migratory insertion in the Cativa process, and halide abstractors can be used to achieve high activity.<sup>4–7</sup> In our prior work with pincer–crown ether ligands, we also observed CO insertion in cationic species  $[\kappa^4-(^{15}C_5)NCOP]Ir(^{13}CH_3)-(CO)]^+$  was  $\sim 11$ -fold faster than in neutral iodide species  $\kappa^3-(^{15}C_5)NCOP]Ir(^{13}CH_3)(CO)(I)$ .<sup>23</sup>

To directly assess migratory insertion at a cationic species, we generated a cationic dicarbonyl complex and examined acetyl formation reactivity. The cationic bis(carbonyl) species

with  $\text{BAR}_4^{\text{F}-}$  anion ( $\text{Ar}^{\text{F}} = 3,5\text{-bis(trifluoromethyl)phenyl}$ ),  $[(^{\text{MeO-Et}}\text{NCOP})\text{Ir}(\text{CH}_3)(\text{CO})_2][\text{BAR}_4^{\text{F}-}]$  ( $[7][\text{BAR}_4^{\text{F}-}]$ ), was synthesized from the reaction of **4-cis** with  $\text{NaBAR}_4^{\text{F}}$  under a CO atmosphere (Scheme 4).  $\text{CD}_2\text{Cl}_2$  solutions of  $[7][\text{BAR}_4^{\text{F}-}]$

#### Scheme 4. Generation of Acetyl via Cationic Species Formation



display a methyl resonance at  $\delta -8.57$  (d,  $J_{\text{PC}} = 6.8$  Hz) in  $^1\text{H}$  NMR spectra and two carbonyl resonances at  $\delta 171.54$  (s) and  $167.41$  (d,  $J_{\text{PC}} = 5.4$  Hz) in  $^{13}\text{C}$  NMR spectra. The CO stretching frequencies of  $[7][\text{BAR}_4^{\text{F}-}]$  observed by IR spectroscopy ( $\nu_{\text{CO}} = 2105, 2064 \text{ cm}^{-1}$ ) are higher energy than those of **4-cis** ( $2023 \text{ cm}^{-1}$ ) and **5-cis** ( $2015 \text{ cm}^{-1}$ ), confirming that the carbonyl ligands are more electrophilic in  $[7]^+$ .

The cationic species  $[7][\text{BAR}_4^{\text{F}-}]$  underwent CO insertion in acetonitrile, as predicted.<sup>23</sup> Thermolysis of  $[7][\text{BAR}_4^{\text{F}-}]$  in  $\text{CD}_3\text{CN}$  at  $80^\circ\text{C}$  under 1 atm of CO for 10 h resulted in  $\sim 60\%$  yield of a new species ( $^{31}\text{P}\{^1\text{H}\}$  NMR  $\delta 141.61$ ) with a diagnostic acetyl peak ( $^1\text{H}$  NMR  $\delta 1.82$ , s) indicative of  $[(^{\text{MeO-Et}}\text{NCOP})\text{Ir}(\text{COCH}_3)(\text{CO})_2][\text{BAR}_4^{\text{F}-}]$  ( $[8][\text{BAR}_4^{\text{F}-}]$ ). Unfortunately, we were unable to isolate  $[8][\text{BAR}_4^{\text{F}-}]$  because removal of the CO atmosphere resulted in reversion to  $[7][\text{BAR}_4^{\text{F}-}]$  (Scheme 4).

The combined results are consistent with acetyl formation requiring acetate dissociation to reach a cationic intermediate capable of CO migratory insertion. Accordingly, only 25% conversion of  $[7][\text{BAR}_4^{\text{F}-}]$  to  $[8][\text{BAR}_4^{\text{F}-}]$  was observed in the presence of (mostly insoluble)  $\text{LiOAc}$  in  $\text{CD}_3\text{CN}$  under 1 atm of CO over 50 h at  $80^\circ\text{C}$ . Complete inhibition of migratory insertion is observed in the presence of tetrabutylammonium acetate, with immediate formation of **4-cis** and **4-trans** and no detectable  $[8][\text{BAR}_4^{\text{F}-}]$ . Whereas these data show that acetate binds strongly to iridium in acetonitrile (acetate dissociation is unfavorable), acetate dissociation to produce cationic iridium species is much more facile in methanol. In fact,  $[7][\text{OAc}]$  formed *in situ* in methanol under CO has almost identical spectral features to  $[7][\text{BAR}_4^{\text{F}-}]$  in methanol. Formation of the cationic dicarbonyl complex enables rapid migratory insertion.

**Comparing Acetate and Iodide Ligands in CO Insertion and Methyl Acetate Formation.** Little is known about how migratory insertion and organic acetyl liberation will change based on the presence of iodide or acetate ligands, but differences in reactivity in these later steps of the proposed catalytic cycle could be important in iodide-free carbonylation processes. In fact, there is relatively little mechanistic information about any reductive elimination

processes relevant to methanol carbonylation,<sup>3,25–27</sup> and some reports point to methanolysis while others propose C–I reductive elimination to produce acetyl iodide as an intermediate.<sup>3,25–27,36,37</sup>

The reactivity of iodide species **5-cis** was examined under CO to compare with the previously described reactivity of acetate complex **4-cis**. Because of poor solubility of **5-cis** in  $\text{CD}_3\text{OD}$ , **5-cis** was dissolved in a mixture of 90%  $\text{CD}_3\text{OD}$  and 10% 1,2-dichloroethane (DCE) and charged with 1 atm of CO. At ambient temperature, relatively little iodide dissociation was observed. After 24 h the mixture comprised unreacted **5-cis**, the isomer where the CO is *trans* to methyl ( $^{\text{MeO-Et}}\text{NCOP})\text{Ir}(\text{CH}_3)(\text{I})(\text{CO})$  (**5-trans**), and  $\sim 40\%$  yield of  $[7]^+$ . This contrasts the behavior of **4-cis**, which generated 70% yield of  $[7]^+$  after only 5 h (*vide supra*), indicating that iodide dissociation is less favorable than acetate dissociation in methanol solvent. Heating this mixture for 3 h at  $65^\circ\text{C}$  led to  $\sim 40\%$  conversion to two iridium carbonyl products, **6** and iridium(III) hydridoiodide species ( $^{\text{MeO-Et}}\text{NCOP})\text{Ir}(\text{H})(\text{CO})\text{I}$  (**9**), identified by a hydride resonance in the  $^1\text{H}$  NMR spectrum ( $\delta -16.64$ , d,  $J_{\text{PH}} = 19.4$  Hz), in an  $\sim 1:8$  ratio. The formation of hydridoiodide **9** is similar to our previous study of a crown-ether-containing iodide complex<sup>22</sup> but contrasts the reactivity of **4-cis** to produce only iridium(I) carbonyl **6**. This raises the possibility that one role of iodide is to shift speciation away from iridium(I) carbonyl, which could have important implications in catalysis. For example, hydride complexes are proposed to be responsible for catalyzing the undesired water-gas shift reaction as a side-reaction during the Cativa process.<sup>1,3,26,38</sup>

To better compare the influence of acetate and iodide ligands on acetyl formation, the kinetics of CO insertion of iodide (**5-cis**) and acetate (**4-cis**) complexes were studied. The kinetics were first compared in  $\text{CD}_3\text{OD}/\text{DCE}$  (8:2) solution, since **5-cis** is insoluble in pure methanol (Table 1). Samples

**Table 1. Half-Lives ( $t_{1/2}$ , min) for Conversion of **4-cis**, **5-cis**, and  $[7][\text{BAR}_4^{\text{F}-}]$  under 1 atm of CO in Methanol<sup>a</sup>**

| solvent                                 | half-life for conversion (min) |                           |                                 |
|---|--------------------------------|---------------------------|---------------------------------|
|   | <b>5-cis</b> <sup>b</sup>      | <b>4-cis</b> <sup>b</sup> | $[7][\text{BAR}_4^{\text{F}-}]$ |
| $\text{CD}_3\text{OD}/\text{DCE}$ (8:2) | 250(10)                        | 120(10)                   | 140(30)                         |
| $\text{CD}_3\text{OD}/\text{DCE}$ (9:1) | 270 <sup>c</sup>               | 72                        | 120                             |
| $\text{CD}_3\text{OD}$ only             | – <sup>c</sup>                 | 69                        | 95                              |

<sup>a</sup>Reactions were heated at  $65^\circ\text{C}$  and monitored by  $^1\text{H}$  and  $^{31}\text{P}\{^1\text{H}\}$  NMR ( $25^\circ\text{C}$ ); based on standard deviation of two trials in  $\text{CD}_3\text{OD}/\text{DCE}$  (8:2), the expected uncertainty for other conditions is  $\pm 10\%$ . Half-life ( $t_{1/2}$ ) is the time to 50% conversion based on an exponential fit of the decaying signal for the Ir–methyl complex (first  $\sim 35\%$  conversion; see the Experimental Section for details). <sup>b</sup>The inverse-gated  $^{31}\text{P}\{^1\text{H}\}$  NMR integrals for each methyl species disappearing was summed to a single integral and plotted to obtain a weighted average half-life. <sup>c</sup>**5-cis** is insoluble in MeOH only.

containing 16 mM Ir were prepared in the glovebox, charged with 1 atm of CO, and heated at  $65^\circ\text{C}$ . The reaction progress was followed by  $^1\text{H}$  and  $^{31}\text{P}\{^1\text{H}\}$  NMR spectroscopy. Because the Ir iodide and acetate complexes establish an equilibrium mixture of *cis/trans* isomers and the dicarbonyl cation  $[7]^+$  under CO in MeOH, the total amount of methyl species was used to evaluate the half-life under pseudo-first-order conditions (see the Supporting Information for details).

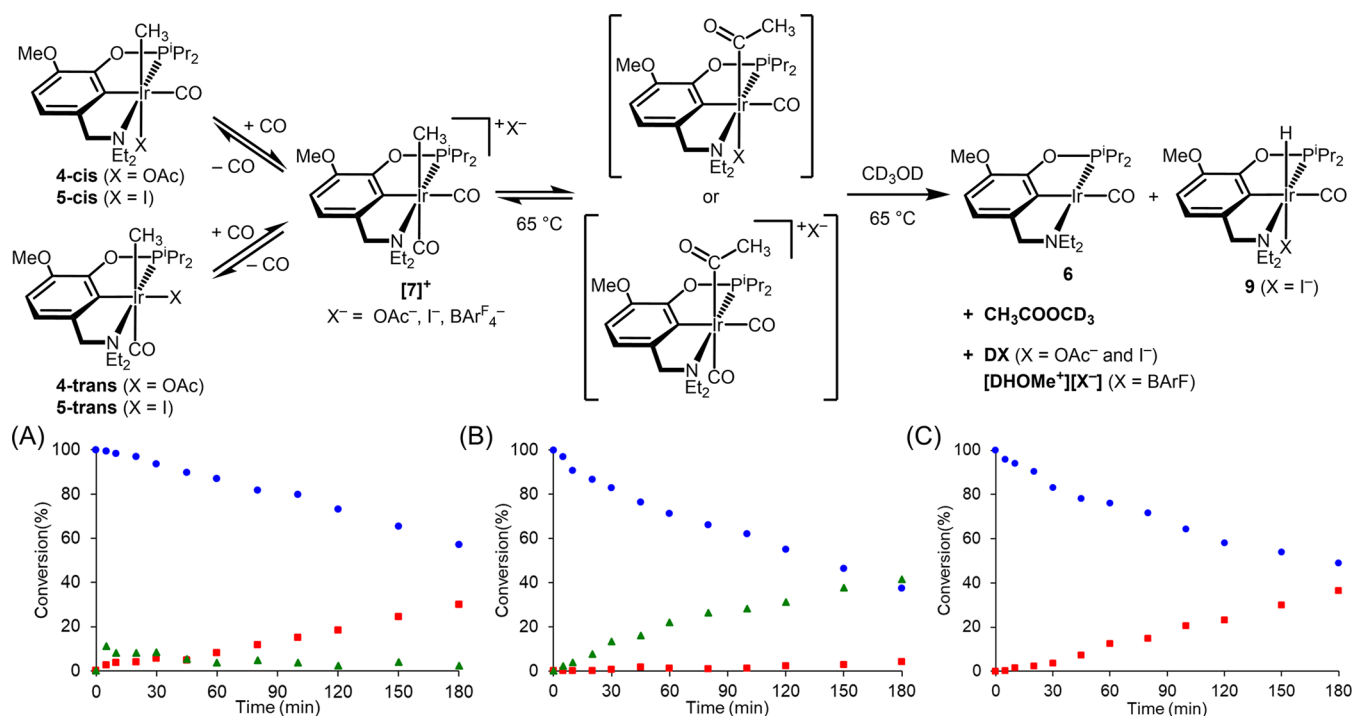


**Figure 5.** Kinetics of CO insertion and reductive elimination with (A) 5-cis, (B) 4-cis, and (C) [7][BARF<sub>4</sub><sup>-</sup>] in CD<sub>3</sub>OD/DCE (8:2) solution. Consumption of sum of the methyl species (blue circles) and yields of the final carbonyl species (red squares) and the acetyl intermediate (green triangles) is shown.

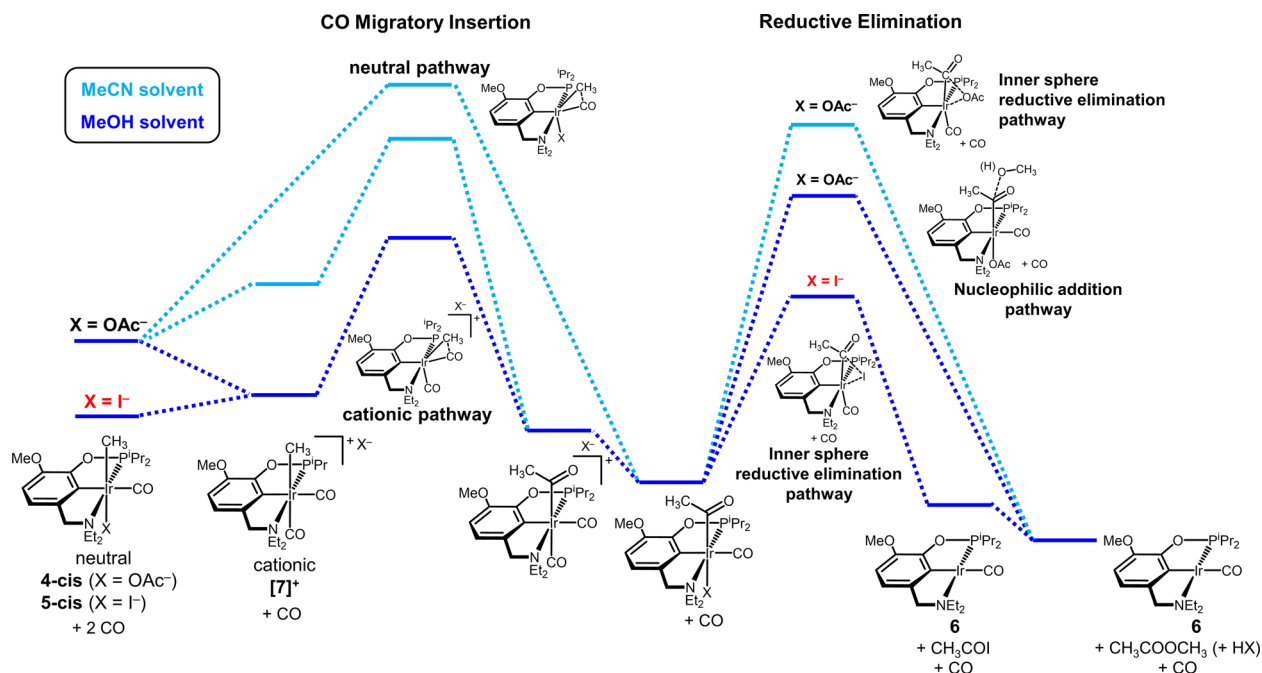


**Figure 6.** Free energy landscape of carbonylation of iridium-methyl compounds comparing effect of anion and solvent.

The iodide species (a mixture of 5-cis, 5-trans, and [7][I]) were consumed with  $t_{1/2} = 250$  min, as the two Ir carbonyl products 6 and 9 appeared (Figure 5A). Only a small amount of an Ir acetyl intermediate (<sup>31</sup>P{<sup>1</sup>H} NMR  $\delta$  140.46) was present during the reaction. This suggests a two-step sequence in which the initial migratory insertion is the rate-determining step.

The acetate species (a mixture of 4-cis, 4-trans, and [7][OAc]) were consumed at a significantly faster rate,  $t_{1/2} =$

120 min (Figure 5B). The reaction forms large amounts of an Ir acetyl intermediate (<sup>31</sup>P{<sup>1</sup>H} NMR  $\delta$  141.92, <sup>1</sup>H NMR  $\delta$  1.81), before giving way to the product 6, acetic acid, and methyl acetate after prolonged heating (*vide supra*). Here, reductive elimination of methyl acetate is the rate-determining step, but the distinct rates of each step enable independent kinetic analysis of the initial migratory insertion step.

The slower rate of migratory insertion of iodide complex 5-cis relative to acetate complex 4-cis is consistent with the lesser

degree of iodide dissociation relative to acetate dissociation observed for this complex, which limits access to the needed cationic intermediate  $[7]^+$  for CO insertion. The trend is opposite for the reductive elimination step, however, with the iodide complex supporting faster methyl acetate formation. The difference could be due to a lower barrier kinetic pathway for formation of acetyl iodide as an intermediate that reacts with methanol to produce methyl acetate, as is typically proposed in the Cativa process.<sup>1–5</sup> The labeling study above (see Scheme 3) established that reactions starting from acetate complex **4-cis** produce methyl acetate directly via coupling of methanol and the acetyl. Consistent with this hypothesis,<sup>25</sup> the reaction of **4-cis** proceeded faster as the methanol content was increased (Table 1), entering a regime where the second step starts to influence the rate of methyl–iridium complex conversion, reaching a maximum in pure CD<sub>3</sub>OD,  $t_{1/2} = 69$  min. No such methanol promotion is observed for the iodide complex, which is more consistent with an iodide/ acetyl reductive elimination pathway.

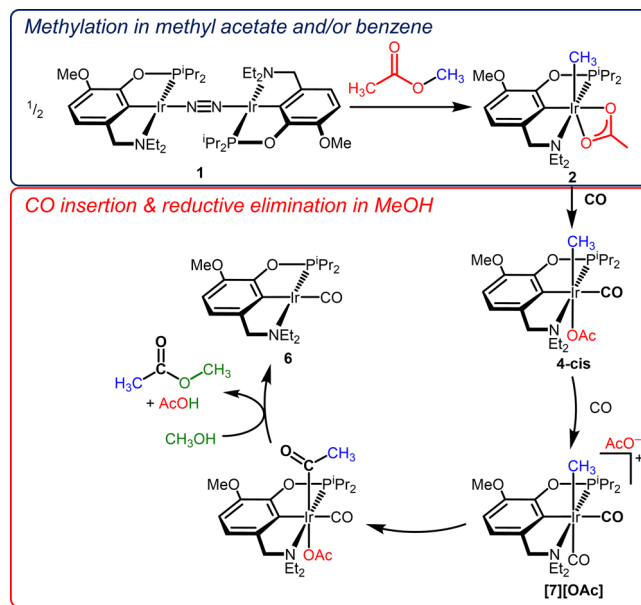
If the faster rate of migratory insertion of acetate complex **4-cis** is due to accessing a cationic dicarbonyl intermediate, the cationic species with a  $\text{BAR}^{\text{F}}_4$  counteranion,  $[7][\text{BAR}^{\text{F}}_4]$ , should exhibit similar kinetics. As shown in Figure 5C,  $[7][\text{BAR}^{\text{F}}_4]$  was consumed at almost the same rate as **4-cis**, consistent with our prediction ( $t_{1/2}$  of 140 min). This is consistent with migratory insertion from similar cationic species  $[7]^+$  in both cases. Surprisingly, however, no acetyl intermediate was observed, and the reaction promptly generated Ir carbonyl product **6**. Methanol is again indicated to be the nucleophile, based on faster rates with higher methanol content (Table 1). The faster rate of reductive elimination in  $[7][\text{BAR}^{\text{F}}_4]$  may be rationalized by the lack of coordinating anion: DFT calculations suggest the acetyl intermediate derived from **4-cis** rebinds acetate, which would slow down reductive elimination relative to the cationic acetyl derived from  $[7][\text{BAR}^{\text{F}}_4]$  (Figure 6). Acetate binding *trans* to the acetyl ligand is ca. 8 kcal/mol more favorable than acetate binding *trans* to the methyl ligand (Tables S12 and S14), suggesting that while acetate dissociation to form a cationic methyl complex is accessible, rebinding of acetate after migratory insertion may inhibit methyl acetate formation.

Figure 6 summarizes the anion and solvent effects on CO migratory insertion and reductive elimination. Methanol solvation promotes acetate dissociation from **4-cis** to produce a cationic methyl species  $[7]^+$  that has a much lower activation barrier for CO migratory insertion than the neutral pathway. Iodide ions inhibit migratory insertion according to the same principles due to preferential halide association to the iridium center that inhibits access to key intermediate  $[7]^+$ . Methanol solvent is also essential for methyl acetate reductive elimination, via either a concerted inner sphere mechanism producing acetyl iodide that reacts with methanol or an outer-sphere nucleophilic addition mechanism. The acetate complex is proposed to undergo outer-sphere reductive elimination by methanol addition to a cationic acetyl intermediate, as indicated by labeling studies and the observation that methyl acetate is produced more rapidly with  $[7][\text{BAR}^{\text{F}}_4]$ . In the presence of iodide, methyl acetate formation is faster, which we attribute to accessing an inner sphere C–I reductive elimination mechanism.

## CONCLUSIONS

An iodide-free carbonylation reaction sequence is reported, based on net C–O bond activation of methyl acetate by a pincer iridium(I) complex followed by CO insertion and formation of acetic acid and another equivalent of methyl acetate (Scheme 5). The net reaction is methanol carbon-

**Scheme 5. Summary of the Carbonylation Reaction via Methyl Acetate C–O Activation**



ylation to acetic acid, with methyl acetate acting as a methylating promoter (and with additional conversion of an iridium(I)–dinitrogen complex to an iridium(I)–carbonyl complex).

The carbonylation sequence provides a unique opportunity to understand how iodide and acetate influence various individual steps relevant to carbonylation catalysis. The CO migratory insertion is strongly solvent dependent. In methanol, acetate complexes undergo fast migratory insertion, attributed to facile acetate substitution by CO to form a cationic dicarbonyl intermediate that facilitates CO insertion. In dichloromethane or acetonitrile, however, CO migratory insertion was not observed, presumably due to unfavorable acetate substitution by CO. The acetate complex undergoes migratory insertion more than twice as fast as the iodide complex in methanol. The faster rate of C–C bond formation with an acetate ligand is attributed to more favorable formation of a cationic methyl dicarbonyl intermediate by acetate substitution relative to iodide substitution in methanol.

Experimental data on acetyl reductive elimination are particularly lacking for iridium-catalyzed carbonylation.<sup>3,25–27</sup> Here, we find evidence for distinct reductive elimination pathways in the presence of acetate and iodide. In methanol solvent, iodide complexes undergo faster elimination than acetate complexes, and the rate does not increase with higher concentrations of methanol. This suggests a direct reductive elimination of acetyl iodide occurs first, followed by reaction with the solvent methanol to generate methyl acetate. In iodide-free conditions, the solvent methanol is the reductive elimination partner, directly generating methyl acetate in a

reaction that proceeds faster when the concentration of methanol increases.

The major current limitation is that the reaction is not catalytic because (a) the resulting iridium(I)–carbonyl complex does not readily react with MeOAc to re-form a methyl–iridium complex and (b) the solvents for methylation and acetylation are incompatible (Scheme 5). Further work is needed to find a system capable of facile activation of methyl acetate in the presence of CO and reaction conditions that can support all the elementary steps of the carbonylation process. Our observations of individual steps in an iodide-free carbonylation scheme may aid in future development of iodide-free carbonylation catalysts and provide rare insight into reductive elimination processes that furnish organic acetyls.

## ASSOCIATED CONTENT

### Supporting Information

The Supporting Information is available free of charge at <https://pubs.acs.org/doi/10.1021/jacs.1c05185>.

Experimental details and characterization data (PDF)  
DFT coordinates (XYZ)

### Accession Codes

CCDC 2084756–2084757 contain the supplementary crystallographic data for this paper. These data can be obtained free of charge via [www.ccdc.cam.ac.uk/data\\_request/cif](http://www.ccdc.cam.ac.uk/data_request/cif), or by emailing [data\\_request@ccdc.cam.ac.uk](mailto:data_request@ccdc.cam.ac.uk), or by contacting The Cambridge Crystallographic Data Centre, 12 Union Road, Cambridge CB2 1EZ, UK; fax: +44 1223 336033.

## AUTHOR INFORMATION

### Corresponding Author

Alexander J. M. Miller – Department of Chemistry, University of North Carolina at Chapel Hill, Chapel Hill, North Carolina 27599-3290, United States; Email: [ajmm@email.unc.edu](mailto:ajmm@email.unc.edu)

### Author

Changho Yoo – Department of Chemistry, University of North Carolina at Chapel Hill, Chapel Hill, North Carolina 27599-3290, United States; Green Carbon Research Center, Korea Research Institute of Chemical Technology (KRICT), Daejeon 34114, Republic of Korea

Complete contact information is available at: <https://pubs.acs.org/10.1021/jacs.1c05185>

### Notes

The authors declare no competing financial interest.

## ACKNOWLEDGMENTS

Eastman Chemical Co. is gratefully acknowledged for financial support. The authors thank Faraj Hasanayn (American University Beirut) for assistance with computational studies and Josh Chen (UNC-CH) for assistance with X-ray crystallography. The NMR spectroscopy was supported by the National Science Foundation under Grants CHE-1828183 and CHE-0922858. The mass spectrometry was supported by the National Science Foundation under Grant CHE-1726291.

## REFERENCES

- (1) Le Berre, C.; Serp, P.; Kalck, P.; Torrence, G. P. Acetic Acid. In *Ullmann's Encyclopedia of Industrial Chemistry*; Wiley-VCH Verlag GmbH & Co. KGaA: Weinheim, Germany, 2014; Vol. 10, pp 1–34.
- (2) Kalck, P.; Le Berre, C.; Serp, P. Recent Advances in the Methanol Carbonylation Reaction into Acetic Acid. *Coord. Chem. Rev.* **2020**, *402*, 213078.
- (3) Morris, G. Carbonylation of Methanol to Acetic Acid and Methyl Acetate to Acetic Anhydride. In *Mechanisms in Homogeneous Catalysis*; Wiley-VCH Verlag GmbH & Co. KGaA: Weinheim, FRG, 2005; Vol. 54, pp 195–230.
- (4) Beller, M.; Steinhoff, B. A.; Zoeller, J. R.; Cole-Hamilton, D. J.; Drent, E.; Wu, X.; Neumann, H.; Ito, S.; Nozaki, K. Carbonylation. In *Applied Homogeneous Catalysis with Organometallic Compounds*; Wiley: Cambridge, 2017; pp 91–190.
- (5) Maitlis, P. M.; Haynes, A.; James, B. R.; Catellani, M.; Chiusoli, G. P. Iodide Effects in Transition Metal Catalyzed Reactions. *Dalton Trans.* **2004**, 3409–3419.
- (6) Haynes, A. Acetic Acid Synthesis by Catalytic Carbonylation of Methanol. In *Catalytic Carbonylation Reactions*; Springer: Berlin, 2006; Vol. 18, pp 179–205.
- (7) Haynes, A.; Maitlis, P. M.; Morris, G. E.; Sunley, G. J.; Adams, H.; Badger, P. W.; Bowers, C. M.; Cook, D. B.; Elliott, P. I. P.; Ghaffar, T.; Green, H.; Griffin, T. R.; Payne, M.; Pearson, J. M.; Taylor, M. J.; Vickers, P. W.; Watt, R. J. Promotion of Iridium-Catalyzed Methanol Carbonylation: Mechanistic Studies of the Cativa Process. *J. Am. Chem. Soc.* **2004**, *126* (9), 2847–2861.
- (8) Bagno, A.; Bukala, J.; Olah, G. A. Chemistry in Superacids. 8. Superacid-Catalyzed Carbonylation of Methane, Methyl Halides, Methyl Alcohol, and Dimethyl Ether to Methyl Acetate and Acetic Acid. *J. Org. Chem.* **1990**, *55* (14), 4284–4289.
- (9) Wegman, R. W. Vapour Phase Carbonylation of Methanol or Dimethyl Ether with Metal-Ion Exchanged Heteropoly Acid Catalysts. *J. Chem. Soc., Chem. Commun.* **1994**, 947.
- (10) Ellis, B.; Howard, M. J.; Joyner, R. W.; Reddy, K. N.; Padley, M. B.; Smith, W. J. Heterogeneous Catalysts for the Direct, Halide-Free Carbonylation of Methanol. *Stud. Surf. Sci. Catal.* **1996**, *101*, 771–779.
- (11) Blasco, T.; Boronat, M.; Concepción, P.; Corma, A.; Law, D.; Vidal-Moya, J. A. Carbonylation of Methanol on Metal-Acid Zeolites: Evidence for a Mechanism Involving a Multisite Active Center. *Angew. Chem., Int. Ed.* **2007**, *46* (21), 3938–3941.
- (12) Boronat, M.; Martínez-Sánchez, C.; Law, D.; Corma, A. Enzyme-like Specificity in Zeolites: A Unique Site Position in Mordenite for Selective Carbonylation of Methanol and Dimethyl Ether with CO. *J. Am. Chem. Soc.* **2008**, *130* (48), 16316–16323.
- (13) Ni, Y.; Shi, L.; Liu, H.; Zhang, W.; Liu, Y.; Zhu, W.; Liu, Z. A Green Route for Methanol Carbonylation. *Catal. Sci. Technol.* **2017**, *7* (20), 4818–4822.
- (14) Meng, X.; Yuan, L.; Guo, H.; Hou, B.; Chen, C.; Sun, D.; Wang, J.; Li, D. Carbonylation of Methanol to Methyl Acetate over Cu/TiO<sub>2</sub>-SiO<sub>2</sub> Catalysts: Influence of Copper Precursors. *Mol. Catal.* **2018**, *456*, 1–9.
- (15) Qi, J.; Christopher, P. Atomically Dispersed Rh Active Sites on Oxide Supports with Controlled Acidity for Gas-Phase Halide-Free Methanol Carbonylation to Acetic Acid. *Ind. Eng. Chem. Res.* **2019**, *58* (28), 12632–12641.
- (16) Tong, C.; Zhang, J.; Chen, W.; Liu, X.; Ye, L.; Yuan, Y. Combined Halide-Free Cu-Based Catalysts with Triple Functions for Heterogeneous Conversion of Methanol into Methyl Acetate. *Catal. Sci. Technol.* **2019**, *9* (21), 6136–6144.
- (17) Zoeller, J. R.; Moore, M. K.; Vetter, A. J. Carbonylation Process. US7582792, 2009.
- (18) Ittel, S. D.; Tolman, C. A.; English, A. D.; Jesson, J. P. The Chemistry of 2-Naphthyl Bis[Bis(Dimethylphosphino)Ethane] Hydride Complexes of Fe, Ru, and Os. 2. Cleavage of sp and sp<sup>3</sup> C-H, C-O, and C-X Bonds. Coupling of Carbon Dioxide and Acetonitrile. *J. Am. Chem. Soc.* **1978**, *100* (24), 7577–7585.
- (19) Trovitch, R. J.; Lobkovsky, E.; Bouwkamp, M. W.; Chirik, P. J. Carbon-Oxygen Bond Cleavage by Bis(Imino)Pyridine Iron Compounds: Catalyst Deactivation Pathways and Observation of Acyl C-O Bond Cleavage in Esters. *Organometallics* **2008**, *27* (23), 6264–6278.

- (20) Manbeck, K. A.; Kundu, S.; Walsh, A. P.; Brennessel, W. W.; Jones, W. D. Carbon-Oxygen Bond Activation in Esters by Platinum(0): Cleavage of the Less Reactive Bond. *Organometallics* **2012**, *31* (14), 5018–5024.
- (21) Kundu, S.; Choi, J.; Wang, D. Y.; Choliy, Y.; Emge, T. J.; Krogh-Jespersen, K.; Goldman, A. S. Cleavage of Ether, Ester, and Tosylate C(sp<sup>3</sup>)-O Bonds by an Iridium Complex, Initiated by Oxidative Addition of C-H Bonds. Experimental and Computational Studies. *J. Am. Chem. Soc.* **2013**, *135* (13), 5127–5143.
- (22) Gregor, L. C.; Grajeda, J.; White, P. S.; Vetter, A. J.; Miller, A. J. M. Salt-Promoted Catalytic Methanol Carbonylation Using Iridium Pincer-Crown Ether Complexes. *Catal. Sci. Technol.* **2018**, *8* (12), 3133–3143.
- (23) Gregor, L. C.; Grajeda, J.; Kita, M. R.; White, P. S.; Vetter, A. J.; Miller, A. J. M. Modulating the Elementary Steps of Methanol Carbonylation by Bridging the Primary and Secondary Coordination Spheres. *Organometallics* **2016**, *35* (17), 3074–3086.
- (24) Yoo, C.; Dodge, H. M.; Farquhar, A. H.; Gardner, K. E.; Miller, A. J. M. Decarbonylative Ether Dissection by Iridium Pincer Complexes. *Chem. Sci.* **2020**, *11* (44), 12130–12138.
- (25) Matsumoto, T.; Mizoroki, T.; Ozaki, A. Mechanistic Study of Methanol Carbonylation Catalyzed by an Iridium Complex in the Presence of Methyl Iodide. *J. Catal.* **1978**, *51* (1), 96–100.
- (26) Forster, D. Kinetic and Spectroscopic Studies of the Carbonylation of Methanol with an Iodide-Promoted Iridium Catalyst. *J. Chem. Soc., Dalton Trans.* **1979**, 1639–1645.
- (27) Kinnunen, T.; Laasonen, K. Reaction Mechanism of the Reductive Elimination in the Catalytic Carbonylation of Methanol. A Density Functional Study. *J. Organomet. Chem.* **2001**, *628* (2), 222–232.
- (28) Choi, J.; Choliy, Y.; Zhang, X.; Emge, T. J.; Krogh-Jespersen, K.; Goldman, A. S. Cleavage of sp<sup>3</sup> C-O Bonds via Oxidative Addition of C-H Bonds. *J. Am. Chem. Soc.* **2009**, *131* (43), 15627–15629.
- (29) Haibach, M. C.; Lease, N.; Goldman, A. S. Catalytic Cleavage of Ether C-O Bonds by Pincer Iridium Complexes. *Angew. Chem., Int. Ed.* **2014**, *53* (38), 10160–10163.
- (30) Chapp, S. M.; Schley, N. D. Evidence for Reversible Cyclometalation in Alkane Dehydrogenation and C-O Bond Cleavage at Iridium Bis(Phosphine) Complexes. *Organometallics* **2017**, *36* (22), 4355–4358.
- (31) Rybtchinski, B.; Vigalok, A.; Ben-David, Y.; Milstein, D. A Room Temperature Direct Metal Insertion into a Nonstrained Carbon-Carbon Bond in Solution. C-C vs C-H Bond Activation. *J. Am. Chem. Soc.* **1996**, *118* (49), 12406–12415.
- (32) van der Boom, M. E.; Liou, S.; Ben-David, Y.; Gozin, M.; Milstein, D. Carbon-Carbon Bond Activation by Rhodium(I) in Solution. Comparison of sp<sup>2</sup>-sp<sup>3</sup> vs sp<sup>3</sup>-sp<sup>3</sup> C-C, C-H vs C-C, and Ar-CH<sub>3</sub> vs Ar-CH<sub>2</sub>CH<sub>3</sub> Activation. *J. Am. Chem. Soc.* **1998**, *120* (51), 13415–13421.
- (33) Rybtchinski, B.; Milstein, D. Metal Insertion into C-C Bonds in Solution. *Angew. Chem., Int. Ed.* **1999**, *38* (7), 870–883.
- (34) Pearson, J. M.; Haynes, A.; Morris, G. E.; Sunley, G. J.; Maitlis, P. M. Dramatic Acceleration of Migratory Insertion in [MeIr(CO)<sub>2</sub>]<sub>3</sub><sup>-</sup> By Methanol and by Tin(II) Iodide. *J. Chem. Soc., Chem. Commun.* **1995**, 1045.
- (35) West, N. M.; Miller, A. J. M.; Labinger, J. A.; Bercaw, J. E. Homogeneous Syngas Conversion. *Coord. Chem. Rev.* **2011**, *255* (7–8), 881–898.
- (36) Lassauque, N.; Davin, T.; Nguyen, D. H.; Adcock, R. J.; Coppel, Y.; Le Berre, C.; Serp, P.; Maron, L.; Kalck, P. Direct Involvement of the Acetato Ligand in the Reductive Elimination Step of Rhodium-Catalyzed Methanol Carbonylation. *Inorg. Chem.* **2012**, *51* (1), 4–6.
- (37) Hanh Nguyen, D.; Lassauque, N.; Vendier, L.; Mallet-Ladeira, S.; Le Berre, C.; Serp, P.; Kalck, P. Reductive Elimination of Anhydrides from Anionic Iodo Acetyl Carboxylato Rhodium Complexes. *Eur. J. Inorg. Chem.* **2014**, *2014* (2), 326–336.
- (38) Elliott, P. I. P.; Haak, S.; Meijer, A. J. H. M.; Sunley, G. J.; Haynes, A. Reactivity of Ir(III) Carbonyl Complexes with Water: